Report

Cell Reports

Mutational Analysis of Measles Virus Suggests Constraints on Antigenic Variation of the Glycoproteins

Graphical Abstract

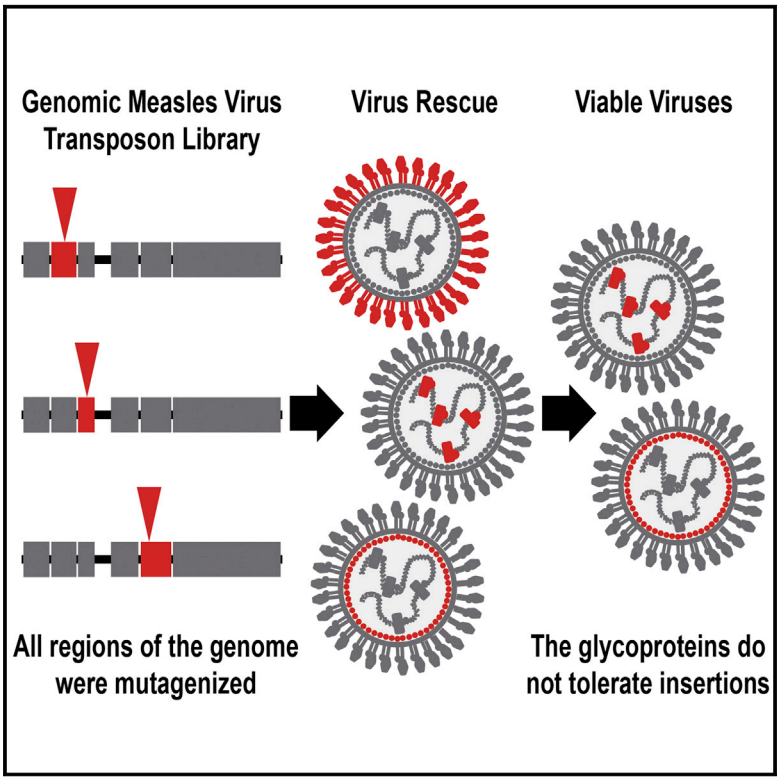

Authors

Benjamin O. Fulton, David Sachs, ..., Peter Palese, Nicholas S. Heaton

Correspondence

nicholas.heaton@mssm.edu

In Brief

It is unclear why measles virus is antigenically monotypic. Fulton et al. perform a viral mutagenesis screen and find that the glycoproteins (the major immune response targets) are exceptionally inflexible. These data suggest that the intrinsic rigidity of the glycoproteins is an important constraint on the development of antigenic diversity.

Highlights

- An insertional mutagenesis screen of the measles virus genome is performed
- Some genomic regions are tolerant of insertions, but the F or H glycoproteins are not
- In comparison to other viruses, the glycoproteins of measles are highly inflexible
- The inflexibility of measles F and H may contribute to measles antigenic stability

Accession Numbers

GSE67666
GSM1653192
GSM1653193
GSM1653194

Fulton et al., 2015, Cell Reports *11*, 1331–1338
June 9, 2015
http://dx.doi.org/10.1016/j.celrep.2015.04.054

Cell Reports
Report

Mutational Analysis of Measles Virus Suggests Constraints on Antigenic Variation of the Glycoproteins

Benjamin O. Fulton,[1] David Sachs,[2] Shannon M. Beaty,[1] Sohui T. Won,[1] Benhur Lee,[1] Peter Palese,[1,3] and Nicholas S. Heaton[1,*]
[1]Department of Microbiology, Icahn School of Medicine at Mount Sinai, New York, NY 10029, USA
[2]Department of Genetics and Genomic Sciences, Icahn School of Medicine at Mount Sinai, New York, NY 10029, USA
[3]Department of Medicine, Icahn School of Medicine at Mount Sinai, New York, NY 10029, USA
*Correspondence: nicholas.heaton@mssm.edu
http://dx.doi.org/10.1016/j.celrep.2015.04.054

SUMMARY

Measles virus undergoes error-prone replication like other RNA viruses, but over time, it has remained antigenically monotypic. The constraints on the virus that prevent the emergence of antigenic variants are unclear. As a first step in understanding this question, we subjected the measles virus genome to unbiased insertional mutagenesis, and viruses that could tolerate insertions were rescued. Only insertions in the nucleoprotein, phosphoprotein, matrix protein, as well as intergenic regions were easily recoverable. Insertions in the glycoproteins of measles virus were severely under-represented in our screen. Host immunity depends on developing neutralizing antibodies to the hemagglutinin and fusion glycoproteins; our analysis suggests that these proteins occupy very little evolutionary space and therefore have difficulty changing in the face of selective pressures. We propose that the inelasticity of these proteins prevents the sequence variation required to escape antibody neutralization in the host, allowing for long-lived immunity after infection with the virus.

INTRODUCTION

Measles virus (MeV) is an enveloped, single-stranded negative-sense RNA virus of the genus *Morbillivirus* in the family *Paramyxoviradae* (Griffin et al., 2012). MeV enters a cell via the actions of two surface glycoproteins, the hemagglutinin (H) and the fusion protein (F) (Yanagi et al., 2006). H acts as the receptor binding protein, whereas F is the actual fusogenic protein responsible for mediating viral envelope and cell membrane fusion (Griffin, 2013). The cellular receptor for MeV is CD150/SLAM; however, some strains (including vaccine strains) can also use the ubiquitously expressed CD46 protein (Yanagi et al., 2009). Neutralizing antibodies against MeV are thought to solely target the F and H proteins, with H being the major neutralizing antigenic target (de Swart et al., 2005). Known to be vaccine preventable, both vaccination and clinical infection confer long-lived immunity (Anders et al., 1996; Moss and Griffin, 2006).

MeV has an error-prone RNA-dependent RNA polymerase (RdRP) that in vitro has a mutation rate similar to that of other RNA viruses (Drake, 1993; Parvin et al., 1986; Sanjuán et al., 2010; Schrag et al., 1999). Over a cycle of infection and transmission between humans, MeV is likely to be exposed to similar selection pressures by the immune system as other respiratory-transmitted viruses (Braciale et al., 2012; Griffin, 1995; Kohlmeier and Woodland, 2009). Therefore, a priori, one might expect that MeV would acquire sequence diversity in surface-exposed protein epitopes to evade the adaptive immune response. Certainly this happens with many viruses, including influenza A virus. However, this antigenic "drift" does not appreciably occur in the MeV F and H glycoproteins. The molecular basis for the lack of emergent antigenically distinct strains of MeV, relative to other related negative-sense RNA viruses like influenza A virus, is currently unclear (Fayolle et al., 1999; Lech et al., 2013; Xu et al., 2013). Given that MeV does not undergo major antigenic changes, it is possible that the glycoproteins of MeV are under a rigid, but as of yet undefined, constraint that prevents this evolution from occurring.

Previously, we reported a 15-nucleotide insertional mutagenesis on the influenza A virus genome (Heaton et al., 2013). Most regions of the influenza A virus genome were found to be resistant to insertion, but the head domain of the hemagglutinin protein was identified as highly tolerant of transposon insertion. We speculated that the observed mutational tolerance was an experimental readout for evolutionary flexible protein domains and that this flexibility was the underlying basis for the rapid antigenic drift observed with influenza A virus. However, we had no comparison to a virus that does not undergo rapid antigenic evolution in its surface glycoproteins.

In this study, we sought to determine where in the antigenically stable MeV genome insertions could be tolerated and, in particular, whether any insertions could be made in the glycoproteins. By performing these experiments under standard cell culture conditions, we asked where MeV had the potential to change in the absence of immune selection. Mutant MeVs with insertions in distinct domains in the nucleoprotein (N), phosphoprotein (P), and matrix protein (M), as well as some intergenic regions, were

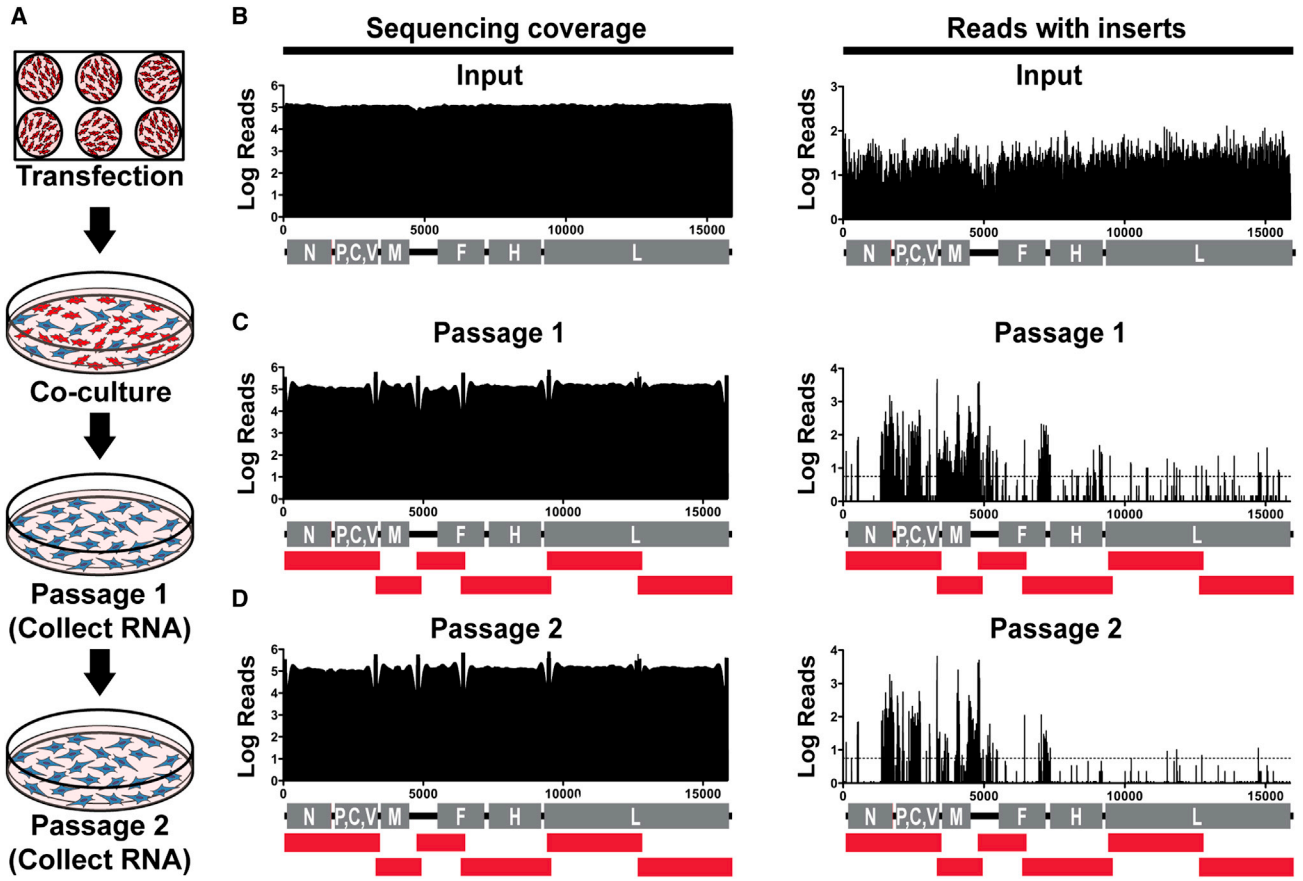

Figure 1. Insertional Mutagenesis of MeV Genome

(A) Mutant viruses were rescued by transfecting BSR-T7 cells with the transposon library and then co-culturing the cells with A549 cells. The resulting viruses were passaged on A549 cells, and viral RNA was sequenced.

(B–D) The input library and both passages were subjected to deep sequencing. The total sequencing coverage of the genome is shown on the left panels, whereas the number of reads containing transposon insertions is indicated on the right. The numbers along the x axis of the graphs indicate the genomic nucleotide position. The red bars under the genome diagrams in (B)–(D) indicate the individual RT-PCR products amplified for Illumina sequencing. Dashed lines indicate a threshold of 0.01% of the total reads.

viable. No MeVs with insertions in either the F or H glycoproteins, or in the large polymerase gene (L), were highly represented in the screen. These data suggest that the MeV hemagglutinin and fusion proteins are very rigid when compared to the influenza A virus hemagglutinin under essentially the same experimental conditions. We hypothesize that this inelasticity may be a contributor to the observed lack of MeV antigenic variation.

RESULTS

Construction and Rescue of the MeV Transposon Library

As a test of viral rescue efficiency, a modified Edmonston strain MeV genomic construct expressing GFP was transfected into BSR-T7 cells with four accessory helper plasmids (Figure S1A). The transfected cells were then co-cultured with permissible human adenocarcinoma alveolar basal epithelial cells (A549s). Passage of viruses on A549s caused large GFP-positive syncytia to form only if all helper plasmids were added to the transfection (Figure S1B). Recovery of infectious particles was high, with the viral titer of MeV GFP after co-culture at 5.2×10^3 TC ID50/ml (Figure S1C).

To generate a high-coverage MeV mutant library, the genome-containing plasmid was mutagenized in vitro with *Mu* transposase and an artificial transposon with a kanamycin selectable marker as previously described (Heaton et al., 2013). The mutagenesis was scaled to generate $>10^5$ individual insertional mutants, which would represent >5-fold coverage of the possible insertion positions. The template for the mutagenesis was a "MeV+3" genomic construct, which does not encode GFP and has an extra three-nucleotide stop codon behind the original stop codon of N (Figure S1D). After mutagenesis and removal of the transposon body, a 15-nt insert remains in the genome (ten of which serve as a unique molecular tag), making the antigenome once again follow the rule of six required by paramyxoviruses (Kolakofsky et al., 1998) (Figure S1E).

To determine where MeV could tolerate insertions, multiple independent rescues of the mutant libraries were performed (Figure 1A). Five days post-transfection, the cells were pooled

and co-cultured with A549s for 3 days to propagate rescued viruses. After co-culture, both supernatant and cell-associated viruses were collected and passaged on fresh A549 cells to select for fully infectious virus mutants (passage 1). The propagated viruses from passage 1 were passaged 72 hr post-infection onto fresh A549 cells for passage 2. RNA extracted from the cells of both passages was subjected to RT-PCR with MeV-specific primers that amplified the genome in six overlapping segments. The subsequent cDNA was prepped and submitted for Illumina HiSeq next-generation sequencing.

Sequencing of our input library demonstrated there was good sequencing coverage and insertions were evenly distributed throughout the MeV genome, with the vast majority of codons containing an insertion (Figure 1B; Table S1). Although the genome of the input library was evenly covered with transposons, only insertions in distinct regions of the MeV genome were recovered after selection (Figures 1C and 1D). Insertion sites in intergenic regions, except those between the H and L genes, were readily recoverable. Sites in the N, P, and M were also abundant. Despite select regions of the MeV genome tolerating insertions, less than 1% of total reads with insertions were detected in the F, H, or L genes. Insertions in the 5′ and 3′ distal un-translated regions (UTRs) of the genome were also only rarely recovered. These data are representative of three independent rescue and passaging experiments.

MeV Surface Glycoproteins Are Intolerant of Insertional Mutagenesis

Analyzing the abundance of insertions across the passages showed that all sites had relatively the same abundance in the input library but were recovered with varying efficiencies (Figure 2A). Viruses rescued in the first round of passaging were generally carried through to the second round in similar proportions, although some were lost or greatly reduced due to additional selection (Figure 2A). We next normalized the percentage of insertions to the size of each genomic region (Figure 2B). The N/P, P/M, and M/F intergenic regions were greatly enriched compared to open reading frames. Although enrichment is seen in N, P, and M, few insertions are seen in the H/L intergenic region or the F, H, and L ORFs.

To validate the screen data, the top insertion sites were cloned into a MeV+3 GFP construct (Figure 2C), rescued, and sequence verified. All of these viruses were easily rescued and formed syncytia on A549 cells similar to the parental virus (Figure 2D; Table 1). The top hits in F, F/H, H, H/L, and L in our screen were also cloned despite the fact that our analysis predicted that they would be significantly attenuated. No viruses were rescuable from the top insertion sites in L and in F (Figure 2D; Table 1). Insertions in sites in the F/H and H/L intergenic regions as well as in H were detectable by fluorescence microscopy after rescue, but viral titer was almost undetectable (Figure 2D; Table 1). Growth curves were then performed on A549 cells with a panel of rescued viruses that grew to sufficiently high titers in the N, P, P/M, M, and M/F regions. We were unable to obtain high-titer viral stocks of H or F protein mutants, so these viruses were excluded from our growth curve analysis. The insertional mutants predicted by our analysis to be viable had only minor attenuation (less than $1\log_{10}$ of TCID50) in multicycle growth relative to the parental MeV (Figure 2E). Therefore, we conclude that the abundance of an insertional mutant detected in our sequencing data is generally correlated with the fitness of the mutant virus.

Analysis of Insertional Mutagenesis of Other RNA Viruses Reveals Exceptional Intolerance of the MeV F and H Glycoproteins

In order to put our MeV insertional mutagenesis into perspective, we took advantage of previously published data sets and analyzed the transposon insertional profiles of influenza A virus (Heaton et al., 2013), hepatitis C virus (HCV) (Remenyi et al., 2014), and Venezuelan equine encephalitis virus (VEEV) (Beitzel et al., 2010) along with our current study on MeV. As each study was performed slightly differently, we plotted each virus individually with each genomic region assigned a value out of a maximum of 1 to show the relative tolerance to insertion. Whereas we observed general consensus on some genomic areas, i.e., polymerase proteins tolerate very few insertions, we observed highly divergent results across the different viral surface glycoproteins responsible for attachment and entry. At one end of the spectrum, the influenza A virus hemagglutinin (HA), and specifically the HA1 domain, which encodes the head region, was the most mutable gene in the entire genome (Figure 3A and inset). VEEV and HCV accepted some insertions in the functionally similar envelope glycoproteins (E2/E1 and E1/E2, respectively) but to a lesser extent than influenza A virus (Figures 3B and 3C). For the HCV E2 glycoprotein, insertions were for the most part limited to the N-terminal hyper-variable region 1 (HVR1) (Hijikata et al., 1991); when analyzed alone, in fact, the HVR1 becomes the second most-tolerant region in the entire genome (Figure 3C, inset). In contrast to the other viruses, strikingly, the MeV F and H glycoproteins were among the most transposon-intolerant genes in the entire MeV genome (Figure 3D).

DISCUSSION

MeV is an antigenically monotypic virus. We began this study in an attempt to gain insight into the molecular basis underlying that phenomenon. Mutagenesis revealed that certain domains of the genome can tolerate insertions. In particular, the intergenic regions toward the 5′ end of the genome were highly enriched for insertions. In addition, certain regions of N, P, and the M genes were also tolerant of mutations. No domains in the glycoproteins or the polymerase genes tolerated insertions, likely due to the effects of the insertion on the structure and therefore function of the gene products.

It is well known that the C terminus of the N protein is one of the most-variable regions across MeV isolates (Xu et al., 1998), with variability also frequently observed in the P gene (Baczko et al., 1992; Bankamp et al., 2008). Previous reports have also shown that MeVs not expressing the M protein, characteristic during subacute sclerosing panencephalitis (SSPE) infections, are viable in vitro (Cathomen et al., 1998). Therefore, it is not surprising that viral mutants with insertions in these genes were frequently recovered during this screen.

Previous studies have shown that the insertion of GFP into the MeV L (Duprex et al., 2002) as well as insertions at the end of the H protein (Hammond et al., 2001; Nakamura et al., 2005; Plemper et al., 2002; Schneider et al., 2000) are viable. We did not

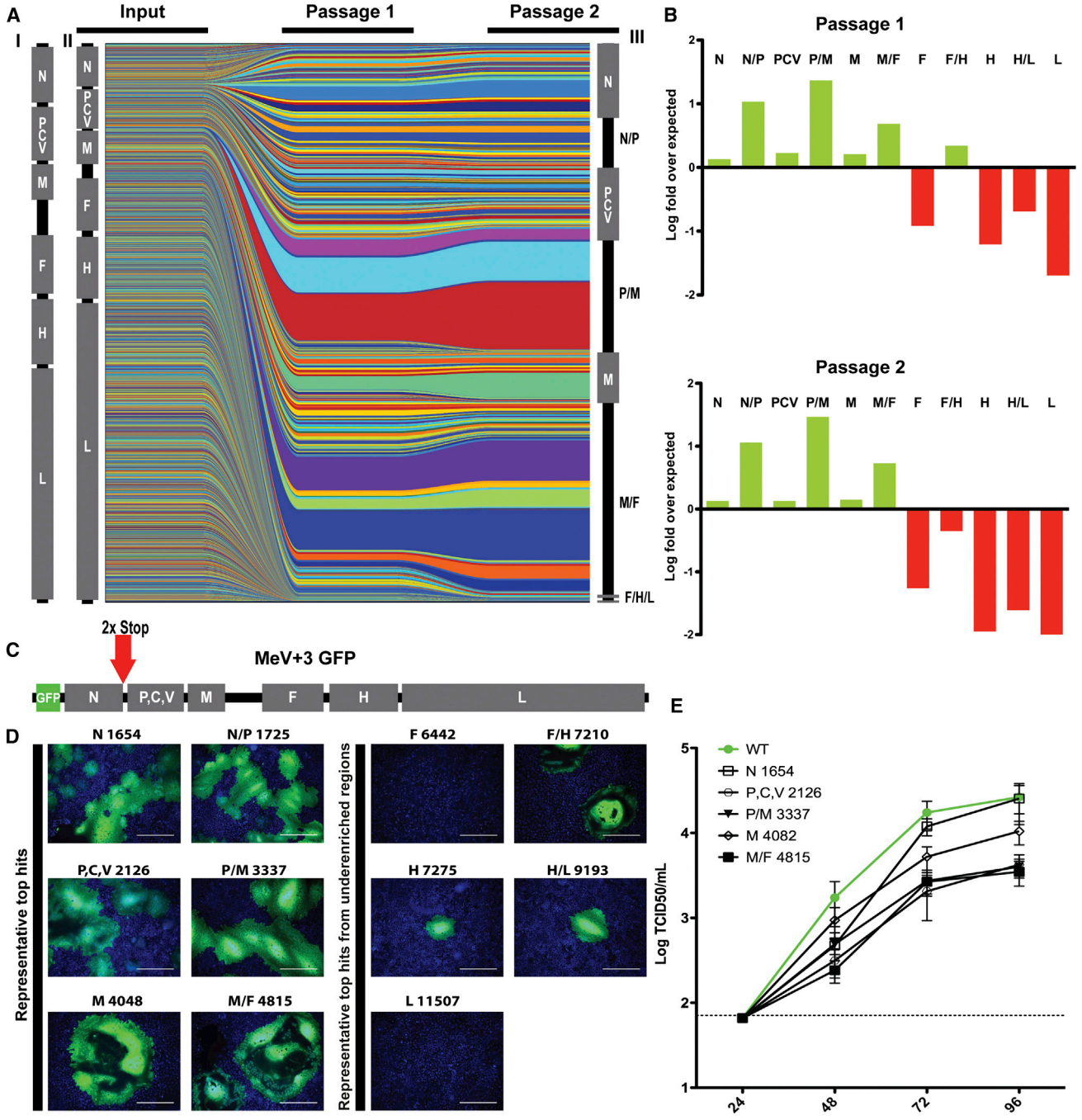

Figure 2. MeV Glycoproteins and Polymerase Genes Are Intolerant of Insertions

(A) Plots representing individual insertion sites. Individual viruses in the input and the passages are represented by different colors; the thickness of the lines is representative of the proportion in the population. The MeV genomes are drawn either to scale (I), distorted to represent the actual coverage of insertions in the input (II), or distorted to represent the total percentage of reads in each region after the second passage (III).

(B) Percent of reads in a region divided by the size of that region to give the fold over predicted values (as if there was no biological selection). Under-represented areas are displayed as negative values (red) whereas over-represented areas are displayed as positive values (green).

(C) Individual insertion sites were cloned into a MeV+3 GFP construct to validate the sequencing results. 2× Stop indicates the presence of an additional stop codon after the normal stop codon of the N gene.

(D) Top hits for the screen, plus the top hits for each region were cloned and rescued. For each panel title, the letter represents the genomic region whereas the number represents the genomic nucleotide position preceding the insertion. The scale bar represents 400 μm.

(E) Growth curves of viruses with insertions in the indicated sites. Values and error bars represent the mean and SEM, respectively. Green filled circles and line, parental MeV.

Table 1. Verified Recoverable Transposon Insertion Sites

Genomic Location	Genomic Nucleotide Position	Codon Preceding Insertion	Translation of Insert	Rescue Titer (Log Fold over MeV +3)
N	1,654	515	IAAAPI	+++
N	1,660	517	YAAAVY	++
N/P	1,720	NA	NA	++
N/P	1,721	NA	NA	++
N/P	1,725	NA	NA	++
P/C/V	2,126	105	GAAATG	++
P/V	2,703	298	CGRTQ	++
P	3,329	506	NAAAMK	++
P/M	3,334	NA	NA	+
P/M	3,337	NA	NA	++
M	4,048	202	GAAAPG	++
M	4,082	214	CGRTE	+++
M/F	4,789	NA	NA	++
M/F	4,801	NA	NA	++
M/F	4,815	NA	NA	+++
M/F	4,826	NA	NA	++
M/F	4,843	NA	NA	+
M/F	4,846	NA	NA	++
F	6,442	330	MRPHSN	-
F	6,953	500	IAAAYI	-
F	7,035	528	CGRKG	-
F/H	7,120	NA	NA	+
F/H	7,210	NA	NA	+
F/H	7,212	NA	NA	+
H	7,275	NA	NA (start codon)	+
H	7,355	27	VRPHRE	+
H	8,697	474	SAAAPR	-
H/L	9,153	NA	NA	-
H/L	9,163	NA	NA	+
H/L	9,193	NA	NA	+
L	11,507	757	CGRNL	-
L	11,846	870	CGRSN	-
L	14,740	1,834	DAAAVE	-

Individual mutant viruses were rescued. The top insertion sites from the screen are shown in the top half of the table. The top three insertion sites in each region from F through L are shown in the bottom half of the table. The titer over the background rescue of the MeV+3 GFP virus was calculated. +++, ≥2logs over background; ++, ≥1log over background; +, ≤1 log over background; -, no virus was detected. N/A indicates the insertion was in a non-coding region.

detect high levels of transposon insertions at those particular locations in our study. This is likely a reflection of multiple factors. First of all, the specific sequence of the insertion likely contributes to the tolerance (or lack of tolerance) of the insertion. Second, the experimental conditions like specific cell lines used for growth of the virus may also change the acceptance of an insertion. Finally, the competitive nature of our viral rescue "hides" some tolerated insertion sites. When all the mutants are rescued and passaged at the same time, only the most-fit viruses are highly represented in the output sequencing. This phenomenon can be observed in the H gene and H/L intergenic region; these areas were significantly under-enriched for transposon insertions in the screen, however, rescue of individual mutants did show some viable (but highly attenuated) viruses (Figure 2D; Table 1). Viral competition shrinking the representation of viable, but attenuated, mutants likely explains why the H gene was devoid of transposons in our study, but variability of H is observed in nature (Bellini and Rota, 1998). We therefore utilize insertional mutagenesis as a readout of generally flexible or inflexible regions of a viral genome, not a comprehensive list of the specific locations that can tolerate insertions. This strategy explores a phenotypic and fitness landscape that is not accessible via normal processes of RdRP-dependent mutation and reveals the most flexible or inflexible regions of the MeV genome.

Whereas wild-type viruses rarely have large insertions or deletions, our data are consistent with the known features of extant MeV strains. For example, distinct MeV strains isolated from clinical infections contained additions in the 3′ UTR of the M gene and deletions in the F 5′ UTR in the M/F intergenic region (Bankamp et al., 2014). Our study showed that this intergenic region contained the most-abundant number of transposons in our screen, totaling ~34% of all reads with insertions.

It is generally accepted that the high sequence diversity frequently associated with RNA viruses is the result of rapid, error-prone replication and strong selection pressures applied by the immune system. However, these factors alone cannot explain why such a large range of antigenic diversity is observed across different RNA viruses. Despite similar viral polymerase error rates and immune system pressures, virus diversity can vary greatly, from antigenically monotypic viruses like MeV to highly drifted viruses like influenza A virus. It stands to reason that evolutionary constraints on the viral protein scaffolds themselves, on which the variation has to arise, could be the missing molecular explanation.

We have provided evidence that, in fact, the glycoproteins of MeV are intolerant of (or highly attenuated by) five amino-acid insertions, which is a fairly significant mutational lesion. When we compare our data set to other RNA viruses mutagenized with the same technique, however, we find that the glycoproteins of VEEV, HCV, and especially influenza A virus tolerate the same five amino acid insertions to a much-greater extent. It is currently unclear why some viral glycoproteins have evolved to be rigid whereas others remain flexible. One possibility is the nature of the receptors utilized by the viruses. Influenza A virus requires only a sialic acid moiety to act as a receptor (Skehel and Wiley, 2000) and is by far the most flexible surface glycoprotein. In contrast, HCV, MeV, and VEEV all utilize at least one proteinaceous receptor (Lindenbach and Rice, 2013; Ludwig et al., 1996; Yanagi et al., 2009), which likely put significant constraints on how flexible the proteins can become. It is also worth noting that the intergenic regions of MeV are highly tolerant to insertions, which may appear to minimize the magnitude of the insertions in the genes themselves. If we exclude the intergenic regions from the analysis, however, the H and F proteins are the second and third least-tolerant open reading frames in the genome, respectively, after the L protein.

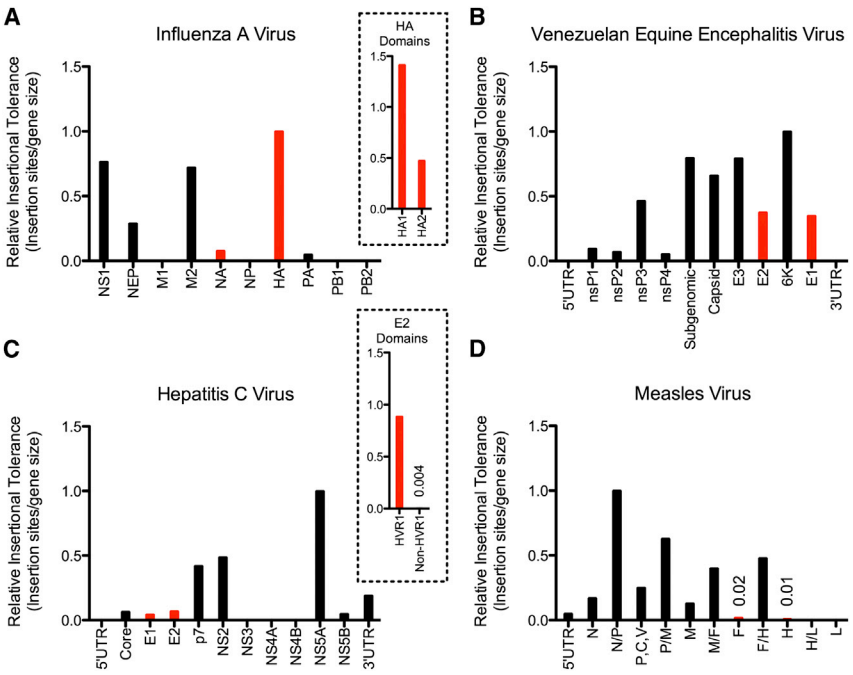

Figure 3. Comparative Analysis Reveals MeV Glycoproteins Are Exceptionally Resistant to Insertional Mutation

The total number of sites that could tolerate insertions in each region were normalized to region size and graphed. Red columns indicate the major viral surface glycoproteins.

(A) Influenza A virus. The HA1 head domain and HA2 stalk domain of the influenza A virus hemagglutinin are separated in the insert.

(B) VEEV.

(C) HCV. The hyper-variable region 1 of E2 is separated from the rest of the E2 protein in the insert.

(D) MeV. All values are out of an arbitrary value of 1.

From a practical standpoint, this technology may allow the prediction of antigenically invariant epitopes in viral proteins for vaccine purposes. Previously, our research demonstrated the HA2 conserved ''stalk'' region of the influenza A virus HA protein was refractory to transposon mutagenesis whereas the head region was very tolerant (Heaton et al., 2013). Work in the influenza A virus vaccine field has found stalk-reactive antibodies to be broadly neutralizing to influenza virus subtypes (Krammer and Palese, 2013), due to a high degree of stalk domain conservation. With respect to MeV, our data predict that the lack of an evolutionary flexible domain in MeV H or F limits the antigenic variation potential of the virus. This may be part of the reason why the MMR live-attenuated vaccine remains effective against currently circulating strains of MeV.

In summary, our data suggest that MeV is antigenically conserved, at least in part, because the H and F proteins themselves are fundamentally unable to tolerate a large range of mutations. This is in contrast to evolutionary flexible proteins like the HA encoded by influenza A virus. The evolutionary constraints imposed by the viral proteins themselves likely represent a key parameter (along with intrinsic viral polymerase mutation rate) in determining long-term viral diversity and potentially the efficacy of a vaccine over long timescales.

EXPERIMENTAL PROCEDURES

Cells

The human alveolar basal epithelial cell (A549) and the baby hamster kidney cell expressing T7 (BSR-T7) cell lines were maintained in DMEM containing 10% FBS by volume and penicillin/streptomycin (Invitrogen).

Generation of MeV Constructs and Viral Rescue

The MeV GFP rescue system was generated by the lab of B.L. using the GFP-N Edmonston antigenomic clone generously provided by W. Paul Duprex (Boston University; Duprex et al., 1999) and heterologous N, P, and L helper genes (a generous gift from Richard Plemper, Georgia State University). See the Supplemental Experimental Procedures for further details.

To test the number of viruses we could rescue from a single transfection, the MeV GFP genomic construct was transfected into BSR-T7 cells with four optimized plasmids expressing codon-optimized T7 polymerase and the N, P, and L helper genes as previously published (Krumm et al., 2013; Radecke et al., 1995). The transfected cells were co-cultured with permissible A549s. Cell-associated and free virus was titered on A549 cells by 50% tissue culture infectious dose (TCID50) as described by Reed and Muench (1938) (Figure S1C). Individual transposon mutant viruses were rescued in a similar manner. Their cloning, rescue, and characterization are fully described in the Supplemental Information.

Generation of MeV Mutant Libraries

A MeV+3 genomic construct suitable for mutagenesis was generated as described in the Supplemental Information. The Mutation Generation System (Fisher Scientific) was used to randomly insert transposons in the MeV+3 plasmid according to the manufacturer's protocol (Figure S1E). Four independent in vitro transposon insertion reactions were performed on 760 ng MeV+3 plasmid, which were then pooled and transformed into Stbl2 cells. Following transformation, the cells were plated on 15-cm plates with LB agar containing ampicillin and kanamycin and allowed to grow for 30 hr at 30°C. The subsequent colonies were scraped and pooled. DNA was extracted from the pooled colonies using a HiPure maxiprep kit (Invitrogen) and digested with NotI (New England Biolabs) to remove the transposon body. The restricted plasmid was then gel purified using the QIAquick kit (QIAGEN), and 1 μg of DNA was re-ligated at 16°C for 16 hr using T4 Ligase (New England Biolabs). The entire ligation mixture was transformed into Stbl2 cells and plated on 15-cm plates containing ampicillin and allowed to grow 30 hr at 30°C. The colonies were again pooled and the DNA was extracted using the HiPure maxiprep kit.

Viral Mutant Library Rescue

The mutant MeV library was rescued using standard protocols with modifications (Krumm et al., 2013; Radecke et al., 1995). 5 μg of MeV genome and four helper plasmids were transfected into 70% confluent BSR-T7 cells in 6-well dishes using the Lipofectamine LTX with Plus (Invitrogen) reagent. A total of five 6-well plates were used for rescuing the viral libraries. At 16 hr post-transfection, the media was replaced with fresh DMEM. Five days post-transfection, the transfected cells were scraped into their media, pooled, and then co-cultured with 60% confluent A549s in 15-cm dishes. After 3 days of co-culture, the cells were again scraped into their media freeze thawed at −80°C and pelleted by centrifugation 4,000 × *g* for 5 min. The clarified supernatant was used to infect 70% confluent A549s in 15-cm dishes. After 3 days (sufficient time to allow high levels of viral replication to occur), the infected cells were

scraped into their media. Half of the cells were pelleted, lysed in 3 ml TRIzol, and frozen at −80°C. The remaining cells were freeze thawed and pelleted by centrifugation (4,000 × *g* for 5 min). The clarified supernatant was again used to infect 70% confluent A549s for a second passage of 3 days in 15-cm dishes. After 3 days, the supernatant was removed and the infected cells were lysed in 6 ml TRIzol and frozen at −80°C.

RT-PCR and Illumina Sequencing

Samples in TRIzol were thawed, and RNA was extracted according to manufacturer's protocols. The MeV genomic RNA was then amplified in six segments using overlapping primers sets as described in the Supplemental Experimental Procedures with Invitrogen's SuperScript III RT-PCR kit with Platinum Taq. The cDNA segments from each sample were pooled in equal molar amounts, sheared with Covaris sonication, and prepped for sequencing using TruSeq DNA LT Sample Prep Kit (Illumina) according to the manufacturer's instructions. Barcoded and multiplexed samples were sequenced on a HiSeq2000 using 100-nt single-end reads in Rapid Run mode.

Analysis of Illumina Sequencing Data

Analysis of the transposon insertions was done as previously described (Heaton et al., 2013). Please see the Supplemental Experimental Procedures for details.

Meta-analysis of HCV, VEEV, and Influenza A Virus Insertional Mutation Data Sets

Previously published data sets were downloaded from the supplemental materials of Beitzel et al. (2010), Heaton et al. (2013) and Remenyi et al. (2014). For VEEV, the 30°C data set was used (Beitzel et al., 2010). For the MeV, HCV, and VEEV data, insertion positions containing >0.01% of total reads were deemed "hits" and divided by the size of the genomic region. For the influenza A virus data, discreet insertion positions in the coding regions (i.e., at least one nucleotide away from a previous "hit" location) ≥9× above background were deemed hits and similarly normalized. For the influenza A virus HA domain analysis, HA1 was defined as the region between nucleotides 81 and 1,121 and HA2 was defined as 1,122–1,730. For the HCV E2 domain analysis, the hyper-variable domain 1 was defined as the first 81 nucleotides of the E2-coding region.

ACCESSION NUMBERS

The raw sequencing data have been deposited and are identified with the following accession numbers at NCBI GEO: GEO:GSE67666, GEO:GSM1653192, GEO:GSM1653193, and GEO:GSM1653194.

SUPPLEMENTAL INFORMATION

Supplemental Information includes Supplemental Experimental Procedures, one figure, and one table and can be found with this article online at http://dx.doi.org/10.1016/j.celrep.2015.04.054.

AUTHOR CONTRIBUTIONS

S.M.B., S.T.W., and B.L. conceptualized, designed, and characterized the measles virus rescue system. B.O.F. and N.S.H. performed the mutagenesis experiments and analyzed data. D.S. performed the bioinformatics analysis of the deep sequencing data. B.O.F., B.L., P.P., and N.S.H. wrote the manuscript.

ACKNOWLEDGMENTS

The authors would like to acknowledge Andrew Varble for his help with the graphical representation of the deep sequencing data. We would also like to acknowledge the genomics and microscopy cores at the Icahn School of Medicine at Mount Sinai. N.S.H. is a Merck fellow of the Life Sciences Research Foundation. S.M.B. was supported by the Viral-Host Pathogenesis Training Grant T32 AI007647. This work was supported in part by the following grants: NIH R21AI115226-01 (to B.L.); R33AI102267-03 (to B.L.); U54AI065359 (to B.L.); U19AI109946-01 (to P.P.); CEIRS HHSN272201400008C (to P.P.); and NIH P01AI097092-02 (to P.P.).

Received: March 11, 2015
Revised: April 22, 2015
Accepted: April 25, 2015
Published: May 21, 2015

REFERENCES

Anders, J.F., Jacobson, R.M., Poland, G.A., Jacobsen, S.J., and Wollan, P.C. (1996). Secondary failure rates of measles vaccines: a metaanalysis of published studies. Pediatr. Infect. Dis. J. *15*, 62–66.

Baczko, K., Pardowitz, I., Rima, B.K., and ter Meulen, V. (1992). Constant and variable regions of measles virus proteins encoded by the nucleocapsid and phosphoprotein genes derived from lytic and persistent viruses. Virology *190*, 469–474.

Bankamp, B., Lopareva, E.N., Kremer, J.R., Tian, Y., Clemens, M.S., Patel, R., Fowlkes, A.L., Kessler, J.R., Muller, C.P., Bellini, W.J., and Rota, P.A. (2008). Genetic variability and mRNA editing frequencies of the phosphoprotein genes of wild-type measles viruses. Virus Res. *135*, 298–306.

Bankamp, B., Liu, C., Rivailler, P., Bera, J., Shrivastava, S., Kirkness, E.F., Bellini, W.J., and Rota, P.A. (2014). Wild-type measles viruses with non-standard genome lengths. PLoS ONE *9*, e95470.

Beitzel, B.F., Bakken, R.R., Smith, J.M., and Schmaljohn, C.S. (2010). High-resolution functional mapping of the venezuelan equine encephalitis virus genome by insertional mutagenesis and massively parallel sequencing. PLoS Pathog. *6*, e1001146.

Bellini, W.J., and Rota, P.A. (1998). Genetic diversity of wild-type measles viruses: implications for global measles elimination programs. Emerg. Infect. Dis. *4*, 29–35.

Braciale, T.J., Sun, J., and Kim, T.S. (2012). Regulating the adaptive immune response to respiratory virus infection. Nat. Rev. Immunol. *12*, 295–305.

Cathomen, T., Mrkic, B., Spehner, D., Drillien, R., Naef, R., Pavlovic, J., Aguzzi, A., Billeter, M.A., and Cattaneo, R. (1998). A matrix-less measles virus is infectious and elicits extensive cell fusion: consequences for propagation in the brain. EMBO J. *17*, 3899–3908.

de Swart, R.L., Yüksel, S., and Osterhaus, A.D. (2005). Relative contributions of measles virus hemagglutinin- and fusion protein-specific serum antibodies to virus neutralization. J. Virol. *79*, 11547–11551.

Drake, J.W. (1993). Rates of spontaneous mutation among RNA viruses. Proc. Natl. Acad. Sci. USA *90*, 4171–4175.

Duprex, W.P., McQuaid, S., Hangartner, L., Billeter, M.A., and Rima, B.K. (1999). Observation of measles virus cell-to-cell spread in astrocytoma cells by using a green fluorescent protein-expressing recombinant virus. J. Virol. *73*, 9568–9575.

Duprex, W.P., Collins, F.M., and Rima, B.K. (2002). Modulating the function of the measles virus RNA-dependent RNA polymerase by insertion of green fluorescent protein into the open reading frame. J. Virol. *76*, 7322–7328.

Fayolle, J., Verrier, B., Buckland, R., and Wild, T.F. (1999). Characterization of a natural mutation in an antigenic site on the fusion protein of measles virus that is involved in neutralization. J. Virol. *73*, 787–790.

Griffin, D.E. (1995). Immune responses during measles virus infection. Curr. Top. Microbiol. Immunol. *191*, 117–134.

Griffin, D.E. (2013). Measles virus. In Fields Virology, Sixth Edition, D.M. Knipe and P.M. Howley, eds. (Philadelphia, PA: Lippincot Williams & Wilkins), pp. 1042–1069.

Griffin, D.E., Lin, W.H., and Pan, C.H. (2012). Measles virus, immune control, and persistence. FEMS Microbiol. Rev. *36*, 649–662.

Hammond, A.L., Plemper, R.K., Zhang, J., Schneider, U., Russell, S.J., and Cattaneo, R. (2001). Single-chain antibody displayed on a recombinant

measles virus confers entry through the tumor-associated carcinoembryonic antigen. J. Virol. *75*, 2087–2096.

Heaton, N.S., Sachs, D., Chen, C.J., Hai, R., and Palese, P. (2013). Genome-wide mutagenesis of influenza virus reveals unique plasticity of the hemagglutinin and NS1 proteins. Proc. Natl. Acad. Sci. USA *110*, 20248–20253.

Hijikata, M., Kato, N., Ootsuyama, Y., Nakagawa, M., Ohkoshi, S., and Shimotohno, K. (1991). Hypervariable regions in the putative glycoprotein of hepatitis C virus. Biochem. Biophys. Res. Commun. *175*, 220–228.

Kohlmeier, J.E., and Woodland, D.L. (2009). Immunity to respiratory viruses. Annu. Rev. Immunol. *27*, 61–82.

Kolakofsky, D., Pelet, T., Garcin, D., Hausmann, S., Curran, J., and Roux, L. (1998). Paramyxovirus RNA synthesis and the requirement for hexamer genome length: the rule of six revisited. J. Virol. *72*, 891–899.

Krammer, F., and Palese, P. (2013). Influenza virus hemagglutinin stalk-based antibodies and vaccines. Curr Opin Virol *3*, 521–530.

Krumm, S.A., Takeda, M., and Plemper, R.K. (2013). The measles virus nucleocapsid protein tail domain is dispensable for viral polymerase recruitment and activity. J. Biol. Chem. *288*, 29943–29953.

Lech, P.J., Tobin, G.J., Bushnell, R., Gutschenritter, E., Pham, L.D., Nace, R., Verhoeyen, E., Cosset, F.L., Muller, C.P., Russell, S.J., and Nara, P.L. (2013). Epitope dampening monotypic measles virus hemagglutinin glycoprotein results in resistance to cocktail of monoclonal antibodies. PLoS ONE *8*, e52306.

Lindenbach, B.D., and Rice, C.M. (2013). The ins and outs of hepatitis C virus entry and assembly. Nat. Rev. Microbiol. *11*, 688–700.

Ludwig, G.V., Kondig, J.P., and Smith, J.F. (1996). A putative receptor for Venezuelan equine encephalitis virus from mosquito cells. J. Virol. *70*, 5592–5599.

Moss, W.J., and Griffin, D.E. (2006). Global measles elimination. Nat. Rev. Microbiol. *4*, 900–908.

Nakamura, T., Peng, K.W., Harvey, M., Greiner, S., Lorimer, I.A., James, C.D., and Russell, S.J. (2005). Rescue and propagation of fully retargeted oncolytic measles viruses. Nat. Biotechnol. *23*, 209–214.

Parvin, J.D., Moscona, A., Pan, W.T., Leider, J.M., and Palese, P. (1986). Measurement of the mutation rates of animal viruses: influenza A virus and poliovirus type 1. J. Virol. *59*, 377–383.

Plemper, R.K., Hammond, A.L., Gerlier, D., Fielding, A.K., and Cattaneo, R. (2002). Strength of envelope protein interaction modulates cytopathicity of measles virus. J. Virol. *76*, 5051–5061.

Radecke, F., Spielhofer, P., Schneider, H., Kaelin, K., Huber, M., Dötsch, C., Christiansen, G., and Billeter, M.A. (1995). Rescue of measles viruses from cloned DNA. EMBO J. *14*, 5773–5784.

Reed, L.J., and Muench, H. (1938). A simple method for estimating fifty percent endpoints. Am. J. Hyg. *27*, 493–497.

Remenyi, R., Qi, H., Su, S.-Y., Chen, Z., Wu, N.C., Arumugaswami, V., Truong, S., Chu, V., Stokelman, T., Lo, H.-H., et al. (2014). A comprehensive functional map of the hepatitis C virus genome provides a resource for probing viral proteins. MBio *5*, e01469–e14.

Sanjuán, R., Nebot, M.R., Chirico, N., Mansky, L.M., and Belshaw, R. (2010). Viral mutation rates. J. Virol. *84*, 9733–9748.

Schneider, U., Bullough, F., Vongpunsawad, S., Russell, S.J., and Cattaneo, R. (2000). Recombinant measles viruses efficiently entering cells through targeted receptors. J. Virol. *74*, 9928–9936.

Schrag, S.J., Rota, P.A., and Bellini, W.J. (1999). Spontaneous mutation rate of measles virus: direct estimation based on mutations conferring monoclonal antibody resistance. J. Virol. *73*, 51–54.

Skehel, J.J., and Wiley, D.C. (2000). Receptor binding and membrane fusion in virus entry: the influenza hemagglutinin. Annu. Rev. Biochem. *69*, 531–569.

Xu, W., Tamin, A., Rota, J.S., Zhang, L., Bellini, W.J., and Rota, P.A. (1998). New genetic group of measles virus isolated in the People's Republic of China. Virus Res. *54*, 147–156.

Xu, S., Zhang, Y., Zhu, Z., Liu, C., Mao, N., Ji, Y., Wang, H., Jiang, X., Li, C., Tang, W., et al. (2013). Genetic characterization of the hemagglutinin genes of wild-type measles virus circulating in china, 1993-2009. PLoS ONE *8*, e73374.

Yanagi, Y., Takeda, M., and Ohno, S. (2006). Measles virus: cellular receptors, tropism and pathogenesis. J. Gen. Virol. *87*, 2767–2779.

Yanagi, Y., Takeda, M., Ohno, S., and Hashiguchi, T. (2009). Measles virus receptors. Curr. Top. Microbiol. Immunol. *329*, 13–30.